ISSN : 0974 - 7486 Volume 8 Issue 10

Trade Science Inc.

Materials Science

An Indian Journal

Full Paper

MSAIJ, 8(10), 2012 [406-417]

High temperature oxidation behaviour of chromium-rich cobalt-based alloys containing high carbides fractions

Patrice Berthod

Institut Jean Lamour (UMR 7198), Team 206 'Surface and Interface, Chemical Reactivity of Materials'
University of Lorraine, Faculty of Science and Technologies B.P. 70239, 54506 Vandoeuvre-lès-Nancy, (FRANCE)
E-mail : Patrice.Berthod@univ-lorraine.fr

Received: 17th March, 2012 ; Accepted: 29th September, 2012

ABSTRACT

Six wear-resistant {30wt.%Cr, 2.5 to 5.0wt.%C} - containing cobalt-based alloys were cast and tested in oxidation by air at 1000, 1100 and 1200°C. The fractions of chromium carbides are especially high and graphite is present but only in the carbon-richest versions, in small quantities. Chromia always exists on the oxidized surfaces, but scales of other oxides, CoO and $CoCr_2O_4$, also appeared. Carbides have disappeared from surface over a depth increasing with the alloy's carbon content and with temperature. The carbide-free depths are higher and the chromium contents on surface are lower for these cobalt alloys than previously observed for similar nickel alloys with the same Cr and C contents. The quantities of chromium and of carbon lost by the oxidized hard cobalt alloys are especially high. All the results show that the behaviours of these cobalt alloys in high temperature oxidation are worse than for the analogous nickel alloys: not really chromia-forming behaviour, faster oxidation, even catastrophic in some cases. The bulk microstructures were either not changed by the high temperature exposures, or only moderately at 1200°C. The hardness of the cobalt alloys is lowered by the exposures to high temperature but remains above the hardness of the similar hard nickel base alloys.

KEYWORDS

Cobalt alloys;
High carbon contents;
Chromium carbides;
Graphite;
High temperature oxidation.

INTRODUCTION

The alloys which are based on cobalt and contain tens of weight percents of chromium are used in various domains. One can meet such alloys in the metallic pieces involved in prostheses for dentistry[1] as well as in aeronautic or power generation components or other hot industrial production machines working at high temperature[2,3]. Some of these alloys also contain carbon which allows obtaining strengthening/hardening carbides of different types, this depending on the carbide-former elements belonging to the chemical composition of the alloy. When chromium is the single carbide-forming element present, several types of carbides can form: $Cr_{23}C_6$, Cr_7C_3, Cr_3C_2 … Such carbides, as well as other carbides involving elements other than chromium, bring the alloy high hardness and high wear-resistance, as in the cutting tools made of a mix of a cobalt-based

binder and numerous dispersed WC carbides present in high fractions[4], or as in the coatings made of Co-W_2C thermally sprayed on steels[5].

The cobalt-based alloys containing high quantities of carbon and chromium may display high levels of resistance against both wear resistance and high temperature corrosion. This results from the obtained high fractions of chromium carbides which behave simultaneously as efficient hardening particles (much more than 1000 Hv[6]) and second as chromium reservoirs able to supply the oxidation front in order to establish and maintain a protective external chromia scale[7]. Concerning especially the later point, and similarly to what was seen earlier about nickel alloys rich in chromium carbides[8], the behaviour in oxidation by air at high temperature (1000°C or more) of materials for wear-resistant applications made on such {chromium carbide} - rich cobalt alloys elaborated by foundry was not so extensively studied as for {WC carbides} – hardened alloys also based on cobalt[9,10].

In this work concerning the high temperature oxidation behaviours of cast alloys very rich in chromium carbides, a set of six cobalt alloys were elaborated by foundry. These alloys, which contain the same high chromium and carbon contents as nickel alloys previously studied[8], were thereafter exposed to air at three high temperatures in order to evaluate their resistance to hot oxidation.

EXPERIMENTAL DETAILS

Choice and synthesis of the alloys

Six compositions {Co-30wt.%Cr} + C with a weight carbon content equal to 2.5 (alloy "Co25"), 3.0 ("Co30"), 3.5 ("Co35"), 4.0 ("Co40"), 4.5 ("Co45") and 5.0wt.% ("Co50") were considered in this study. The work started by performing thermodynamic calculations in order to estimate the theoretic melting range of temperatures and to explore the types of microstructures of these alloys. This was done using the Thermo-Calc software[11] and a database containing the descriptions of the Co–Cr–C system and of its sub-systems[12-17]. These calculations aimed to predict the s

microstructures of the alloys of interest at the temperatures of the oxidation tests, and notably the chromium repartition between matrix and the chromium carbides which can be of great importance for the behaviour of these alloys in high temperature oxidation. Additional calculations were thereafter performed to specify the conditions which must be respected by the local carbon contents to allow a single-phased state of the oxidation-affected subsurface of the oxidized samples.

The alloys were all elaborated using a high frequency induction furnace (CELES) under an atmosphere of 300mbar of argon gas. In each case a mix of pure elements (>99.9%, Alfa Aesar) was melted and solidified in the water-cooled copper crucible of the furnace. This led to ingots of about 40g.

Compact samples of about 125 mm^3 were cut in these ingots to obtain the samples for the three oxidation tests. After surface preparation, these samples were exposed to the laboratory air at 1000, 1100 or 1200°C for 50 hours in a resistive tubular furnace, and thereafter air-cooled to room temperature.

The as-cast samples as well as the oxidized samples were embedded in a cold resin mixture. They were thereafter cut in two parts using a Buehler Isomet 5000 precision saw, and polished. Polishing was performed first with SiC papers under water (up to 1200 grit) and second with 1μm-particles on textile paper. The metallographic observations were done using a Scanning Electron Microscope (SEM, XL30 Philips) in the Back Scattered Electrons mode (BSE) with an acceleration voltage of 20 kV. X-Ray Diffraction performed using a Philips X-Pert Pro diffractometer (wavelength Cu Kα) allowed identifying the carbides' natures at the temperatures of the oxidation tests. WDS profiles (Wavelength Dispersion Spectrometry) were performed using a Cameca SX100 microprobe in order to identify the natures of the oxides formed on the sample surfaces, and to characterize the chromium depletion in the subsurface. Finally, Vickers indentations were carried out using a Testwell Wolpert apparatus (load: 30kg) for detecting and evaluating an eventual loss in hardness of the alloys after the exposures to high temperature.

RESULTS AND DISCUSSION

Results of thermodynamic calculations

Thermodynamic calculations were carried out to

Full Paper

better know the solidification progress and to predict the microstructures stable at high temperature. A first set of calculations showed that only the Co25 and Co30 alloys, i.e. the less rich in carbon among the alloys considered in this study, would behave at solidification as cobalt alloys with classical chromium and carbon contents, as is to say with a first crystallization of matrix dendrites and a final eutectic solidification of matrix and carbides together. In contrast the solidification of the Co35, Co40, Co45 and Co50 alloys should start by the appearance of carbides. For these ones several types of carbides would appear, either during solidification, or during the cooling in solid state: M_7C_3 and cementite.

The as-cast microstructures of the solidified alloys are illustrated by the SEM micrographs presented in Figure 1. The presence of dendrites of matrix in the Co25 alloy, the wholly eutectic microstructure type of the Co30 alloy and the presence, in the four carbon-richest alloys, of acicular carbides much coarser that the eutectic ones, confirm that the first alloy is effectively hypo-eutectic, the second one almost eutectic and the four other ones hyper-eutectic. However, if the comparisons with such calculated results and the microstructures really obtained showed a good qualitative agreement concerning the position of the chemical composition versus the eutectic valley, the existence of the not-predicted graphite in the three carbon-richest alloys (in fact really evidenced in significant quantity only in the Co50 alloy) showed that calculations did not well represent the solidification sequences.

New calculations were performed by suspending the cementite phase (to obstruct its theoretic appearance). They led to a much better agreement: no change for the Co25 and Co30 alloys and graphite appearance in the alloys richer in carbon. These calculations carried out with the suspension of cementite led to the qualitative results presented in TABLE 1. In this table one can see that both austenitic FCC matrix and the M_7C_3 carbides would be present in the alloys with 2.5, 3.0 and 3.5wt.%C at 1000, 1100 and 1200°C,while the microstructures of the alloys containing 4.0, 4.5 and 5.0wt.%C would be composed of FCC matrix, M_7C_3 carbides and also graphite, for the three same temperatures of interest.

More quantitative results of these calculations are presented in TABLE 2. They are focused on matrix: its mass fraction in the alloys and its chromium content in

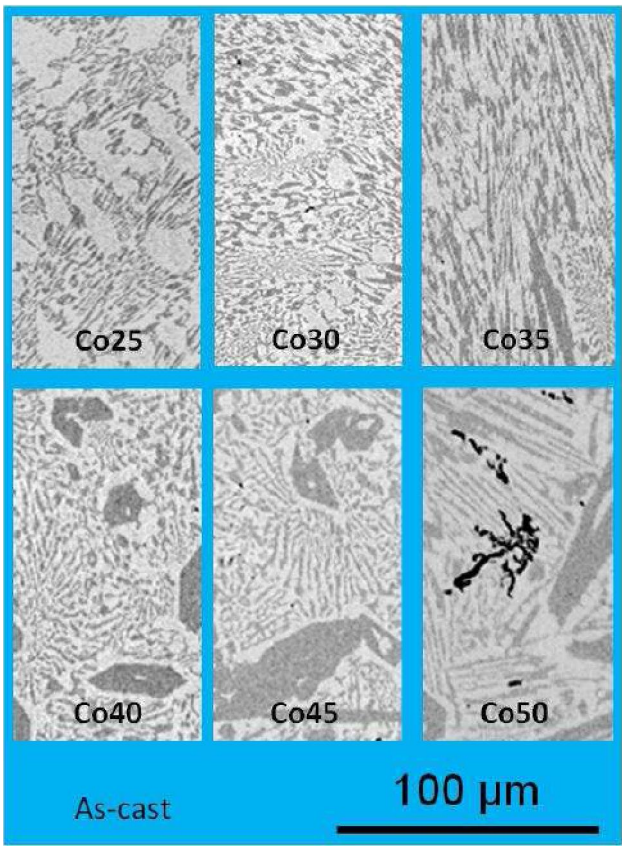

Figure 1 : The as-cast microstructures of the studied cobalt-base alloys

TABLE 1 : Phases present in the microstructures of the studied alloys at the temperatures of the oxidation tests (according to Thermo-Calc)

Phases	1000°C	1100°C	1200°C
Co25	mat.FCC + M_7C_3	mat.FCC + M_7C_3	mat.FCC + M_7C_3
Co30	mat.FCC + M_7C_3	mat.FCC + M_7C_3	mat.FCC + M_7C_3
Co35	mat.FCC + M_7C_3	mat.FCC + M_7C_3	mat.FCC + M_7C_3
Co40	mat.FCC + M_7C_3 + graphite	mat.FCC + M_7C_3 + graphite	mat.FCC + M_7C_3 + graphite
Co45	mat.FCC + M_7C_3 + graphite	mat.FCC + M_7C_3 + graphite	mat.FCC + M_7C_3 + graphite
Co50	mat.FCC + M_7C_3 + graphite	mat.FCC + M_7C_3 + graphite	mat.FCC + M_7C_3 + graphite

the stable state, at each of the three temperatures of the oxidation tests. For a given alloy, when the temperature increases the mass fraction of matrix increases as well as its chromium content. For a given temperature both matrix mass fraction and matrix chromium content decrease when the alloy becomes richer and richer in carbon. These decreases in mass fraction of matrix and in chromium content in matrix with the increase in carbon content in the alloy are significant until the presence of graphite. Indeed, for the alloys Co40, Co45 and especially Co50, for a same temperature the mass fraction of matrix decreases slowly and its chromium content is constant, according to Thermo-Calc.

It can be pointed out that the matrix, which represents three-quarters of the whole alloy in Co25 at 1200°C and contains about 15wt.%Cr, would be only almost half the alloy mass in Co50 at 1000°C, with a very low chromium content of about 4.4wt.%Cr. Such an imbalance between discrete chromium-rich carbide particles and a chromium-poor continuous metallic phase may greatly influence the oxidation behaviour of the alloy and may lead to very different oxidation resistances for these ternary alloys although they all contain 30wt.% of chromium.

TABLE 2 : Mass fractions and chromium contents of the matrix at the temperatures of the oxidation tests (according to Thermo-Calc)

mass.% of matrix	wt.% Cr in matrix	1000°C		1100°C		1200°C	
Co25		72.78	12.63	73.61	13.75	74.77	14.96
Co30		67.36	9.20	68.49	10.74	70.00	12.29
Co35		62.05	6.28	63.63	8.27	65.58	10.13
Co40		57.44	4.38	59.63	6.66	61.86	8.65
Co45		56.90	4.38	59.07	6.66	61.29	8.65
Co50		56.37	4.38	58.51	6.66	60.71	8.65

Metallographic results after the high temperature oxidation tests

The surface states of all the alloys oxidized at 1000, 1100 or 1200°C during 50 hours are illustrated by SEM/BSE micrographs in Figure 2 for the Co25, Co30 and Co35 alloys, and in Figure 3 for the Co40, Co45 and Co50 alloys.

All the samples display external oxide scales. Their quality and integrity are very variable, and the worst ones are the ones covering the oxidized carbon-richest alloys. Chromia is present in all cases, as a continuous

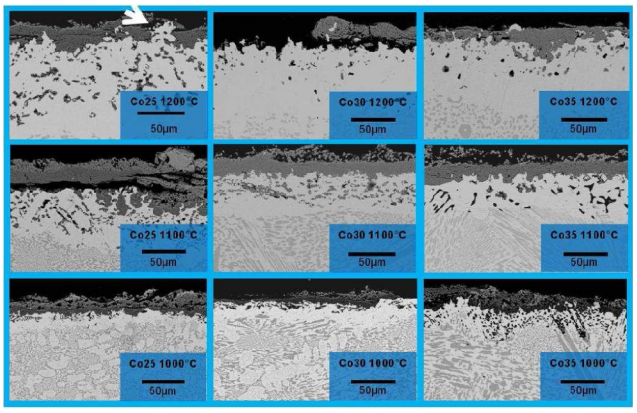

Figure 2 : External oxides scales and sub-surface states of the alloys Co25, Co30 and Co35 after 50h of oxidation in air at 1000, 1100 and 1200°C

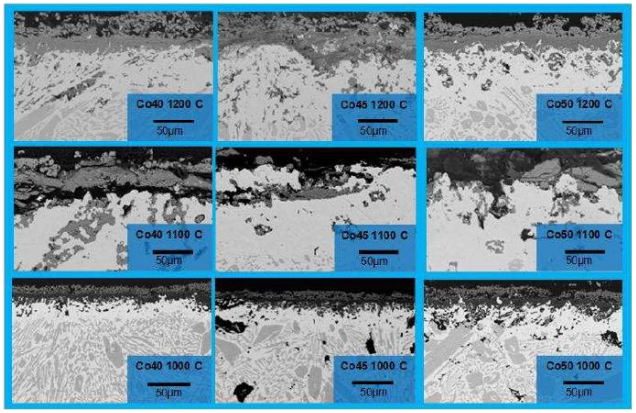

Figure 3 : External oxides scales and sub-surface states of the alloys Co40, Co45 and Co50 after 50h of oxidation in air at 1000, 1100 and 1200°C

scale covering the surfaces of the samples or as internal oxide films in the subsurface, as evidenced by the WDS concentration profiles displayed in Figure 4. In other cases chromia is an internal layer in direct contact with the surface of the sample, which separates the later from a more external layer composed of CoO (more frequent after oxidation at 1000°C) or of spinel oxide $CoCr_2O_4$ (illustrated by the WDS profiles in Figure 5(b)). This spinel oxide can be also the single oxide present on surface (Figure 5(a)). One can notice that the oxide scales over the surfaces of the three C-richest alloys oxidized at 1200°C are especially disordered, by comparison with the other scales observed in all the other cases.

Under these oxide scales the alloys are affected by the loss of their carbides. These ones have either disappeared (case of the fine eutectic carbides and of the not too coarse pro-eutectic carbides) or have been oxi-

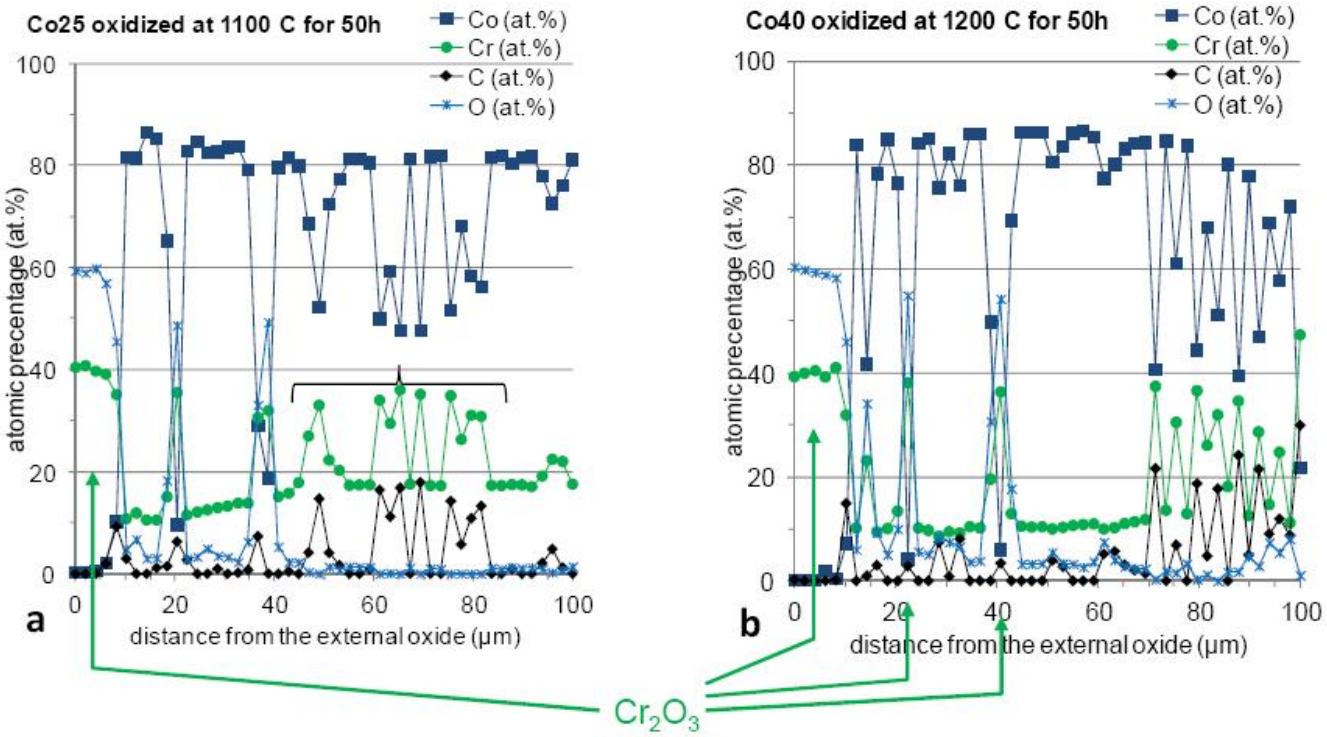

Figure 4 : Concentrations' profiles across the external oxide scale and the sub-surface showing the presence of chromia (a & b) as external oxide scale and as internal oxide films (b)

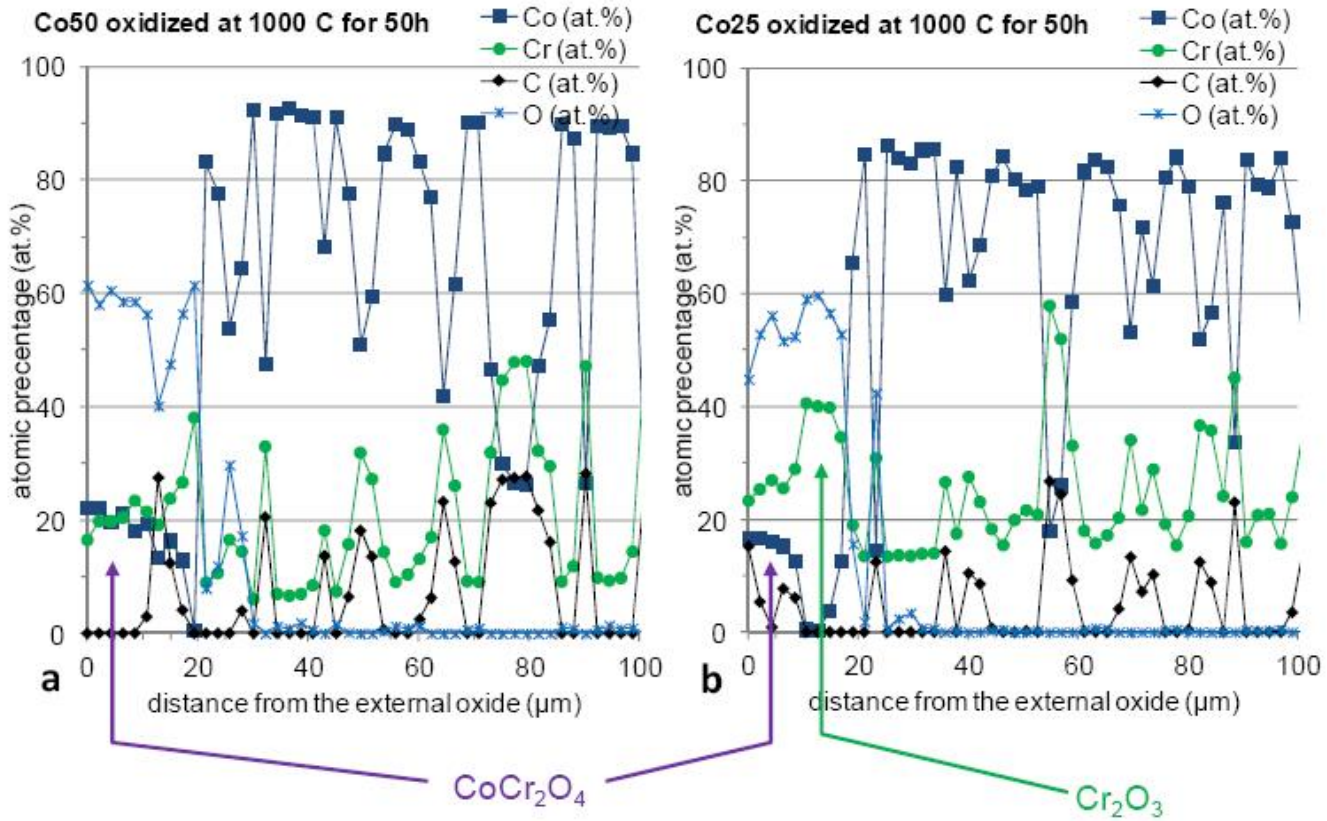

Figure 5 : Other examples of concentrations profiles across the surface and subsurface of oxidized samples; presence of a spinel oxide ($CoCr_2O_4$) as single scale on the surface of some oxidized alloys (a) or over an internal layer of chromia (Cr_2O_3) (b)

dized on site (case of the coarsest pro-eutectic carbides). The carbide-free zones which developed from the surface only contain internal oxides, in more or less great quantities. Their depths were measured and the results, average of three values ± standard deviation, are displayed in TABLE 3. One can see for the Co25, Co30 and Co35 alloys that the carbide-free zone becomes deeper when the oxidation temperature increases from 1000 to 1200°C. This can be also observed, but only between 1000 and 1100°C, for the Co40, Co45 and Co50 alloys. Indeed, for these carbon-richest alloys, the depth over which carbides have disappeared is in contrast lower for 1200°C than for 1100°C. In these two later cases there was obviously a backward movement of the alloy/oxide interface, due to a general oxidation which also explains the very perturbed aspect of the scales. After oxidation at 1000°C all the alloys present the same depth of carbide-free zone. This is also true for the Co25, Co30 and Co35 alloys after oxidation at 1100°C, and for the Co40, Co45 and Co50 alloys after oxidation at this same temperature. However the three later alloys have lost carbides over a depth which is twice the one for the three first alloys. After oxidation at 1200°C, the depth of carbide-free zone decreases when the carbon content increases from 2.5 to 3.5wt.%C, while the three values for the carbon-richest alloys are at the same low level, revealing an alloy consumption.

TABLE 3 : Average depths of the carbide-free zone

Carbide-free zone depth (μm)	1000°C	1100°C	1200°C
Co25	19 ±2	40 ±11	123 ±4
Co30	22 ±3	47 ±2	90 ±13
Co35	20 ±3	39 ±4	84 ±4
Co40	22 ±1	101 ±19	57 ±1
Co45	22 ±3	112 ±10	70 ±7
Co50	27 ±3	92 ±15	64 ±24

WDS concentration profiles were obtained by microprobe across the external oxides and the chromium-depleted sub-surface for all samples. Some examples of the concentration profiles obtained are given in Figure 4 and Figure 5. The first results to consider are the minimal value of chromium content measured on the extreme surface of the alloys, just under the external oxide scales (TABLE 4, in bold characters). One can first notice that these contents are often similar to the ones in the matrix in the bulk at the corresponding temperatures (TABLE 2, in bold characters). They globally show the same tendency of decrease when the alloy's carbon content increases and of increase when the temperature increases. Concerning the later remark about the increase of the chromium content on surface with temperature, the Co40, Co45 and Co50 alloys are to be considered as exceptions since they present, after the oxidation at 1200°C which catastrophically progressed, chromium contents which are much lower than after oxidation at 1100°C.

A little deeper (across the carbide-free zone) the chromium contents are higher, which results from local matrix enrichment in chromium accompanying the dissolution of the carbides at the carbide-free zone frontier. These chromium contents on surface are lower than 15wt.%, and often than 10wt.%, with in addition several values as low as 5wt.%. Such chromium contents are not compatible with a behavior still chromia-forming and this explains the presence of thick spinel scales over a thin chromia layer. In TABLE 4 too the values of the average concentration gradient for chromium across the carbide-free zone are given, to complete the description of chromium distribution in the carbide-free zone. This determination was possible only when the chromium concentrations profiles presented regular parts long enough, as is to say for the alloys after oxidation at 1100 and at 1200°C. The profiles obtained for the alloys oxidized at 1000°C were too perturbed to allow assessing such gradients. The results presented

TABLE 4 : Minimal chromium weight contents near the external surface and average chromium content gradients across the carbide-free zone (one WDS profile per oxidized alloy)

wt.%Cr on surface	average Cr gradient in the cfz (wt.%Cr/μm)	1000°C		1100°C		1200°C	
	Co25	12.4	X	9.6	0.170	15.1	0.052
	Co30	9.9	X	11.0	0.045*	10.6	0.067
	Co35	7.9	X	11.5	0.064	14.6	0.043
	Co40	5.4	X	13.0	0.034	9.0	0.052
	Co45	4.8	X	15.3	0.018	5.5	0.147*
	Co50	5.5	X	10.6	0.052	7.2	0.078

X: not possible to assess Cr gradient *: measurement of Cr gradient not accurate

in TABLE 4 show that there is obviously no systematic dependence of the chromium gradient neither on the carbon content in the alloy, nor on the oxidation temperature.

Balance sheets in chromium and in carbon for the sub-surfaces

With the previous results of WDS measurements (only available for 1100°C and 1200°C) and of carbide-free depth, it is possible to assess the mass of chromium lost by the alloys during oxidation. For each alloy the difference between the average chromium content in the carbide-free zone and 30wt.% (initial content), when it can be assumed that there was no backward movement of the {external oxide / alloy} interface during the oxidation tests (as for Co40, Co45 and Co50 at 1200°C), it is possible to estimate the quantity of chromium having leaved the alloy to form the chromia external scale and eventually the volatile oxide CrO_3. TABLE 5 shows the results, in the form of intervals of values {average ± standard deviation} resulting from the interval of carbide-free zone depth (TABLE 3). In general the mass of chromium lost by the alloys during the 50 hours of oxidation tends increasing from Co25 to Co50, with two types of levels obviously depending on the presence of graphite (about 6 mg/cm² for Co25, Co30 and Co35, and twice this value (about 12.5 mg/cm²) for Co40, Co45 and Co50. The mass of lost chromium also increases with temperature, but only for the Co25, Co30 and Co35 alloys. The values for 1200°C are not higher than the ones for 1100°C for the Co40, Co45 and Co50 alloys. This pointed out an alloy consumption by catastrophic oxidation in that cases, which results in a less deep carbide-free zone and then in an underestimation of the mass of lost chromium.

As in the case of the nickel-based alloys of the first part of this study, the main part of the carbon atoms released by the disappearing carbides have lost the alloys. Here too they cannot exist in great quantities in the carbide-free zone, as it can be demonstrated by thermodynamic calculations[18, 19]. Indeed, Figure 6 presents isothermal sections of the Co-Cr-C diagram computed with Thermo-Calc for 1000, 1100 and 1200°C. These ones show that the carbon contents in the carbide-free zones must be lower than 1wt.% and less, which is much lower than 2.5 to 5wt.% of carbon initially present. Moreover the carbon contents in the carbide-free zones can be considered as negligible since it is extremely probable that these small atoms diffused toward the oxidation front to be oxidized as gaseous species leaving the alloy. This allows assessing the masses of carbon having leaved the alloys, leading to the values presented in TABLE 6. One can see that the mass of carbon lost by the oxidizing alloys increases with the initial carbon content of the alloy, as well as with temperature. Concerning the alloys Co40, Co45 and Co50, the underestimation of the depths of the carbide-free zones, due to alloy consumption and then backward movement of the alloy/oxide interface, led here to underestimated values of the mass of lost carbon (which are even lower than at 1100°C), similarly as what was previously seen about the lost chromium.

Microstructure and hardness evolutions in the bulk

As for the nickel alloys earlier studied[8] such exposures at high temperature during the oxidation test favor modifications in the bulk microstructures of the alloys. However, by comparison with the as-cast microstructures the carbides have not significantly evolved, except for the samples exposed at 1200°C since, qualitatively, their carbides shapes seem to be a little rounder and their carbide surface fractions slightly lower. Changes can be also expected concerning the carbides types, since they may have changed, by comparison to

TABLE 5 : Estimated values of the masses of chromium lost per cm² of external surface by the alloys during oxidation: difference between 30wt.% and the average new Cr content in the carbide-free zone; average and (minimal - maximal) values

Loss of Cr in the carbide-free zone (mg/cm²)	1000°C	1100°C	1200°C
Co25	X	5.77 (4.20-7.33)	12.6 (12.2-13.0)
Co30	X	7.10 (6.84-7.37)*	12.1 (10.3-13.9)
Co35	X	5.28 (4.80-5.75)	9.46 (9.07-9.86)
Co40	X	12.6 (10.2-15.0)	9.20 (9.04-9.36)**
Co45	X	12.3 (11.2-13.4)	11.6 (10.4-12.8)**
Co50	X	12.4 (10.5-14.4)	11.0 (6.9-15.1)**

***: estimation not accurate**: underestimation due to alloy consumption**

the as-cast state, in order to correspond to the thermodynamic equilibria at 1000, 1100 or 1200°C. X-Ray Diffraction spectra were performed on the bulk to identify the stoichiometry of these carbides at these temperatures, assuming that the high temperature stages were long enough for allowing the transformation of the carbides to the most stable ones.

TABLE 6 : Estimated values of the masses of carbon lost per cm² of external surface by the alloys during oxidation, assuming that carbon is negligible in the carbide-free zone by comparison with the initial carbon content; average and (minimal - maximal) values

Loss of C in the carbide-free zone (mg/cm²)	1000°C	1100°C	1200°C
Co25	0.38 (0.35-0.42)	0.80 (0.58-1.02)	2.44 (2.37-2.51)
Co30	0.52 (0.45-0.58)	1.13 (1.09-1.17)	2.15 (1.83-2.46)
Co35	0.57 (0.49-0.64)	1.07 (0.98-1.17)	2.34 (2.25-2.44)
Co40	0.69 (0.66-0.72)	3.22 (2.61-3.83)	1.82 (1.79-1.85)*
Co45	0.77 (0.68-0.87)	4.02 (3.66-4.37)	2.51 (2.26-2.76)*
Co50	1.09 (0.99-1.20)	3.67 (3.09-4.25)	2.56 (1.61-3.51)*

***: underestimation due to alloy consumption**

It was also assumed that the air quenching was strong enough to preserve the high temperature types obtained for these carbides. It appeared that the carbides identified by these experiments are Cr_7C_3 (examples of spectra given in Figure 7 and Figure 8) as predicted by the thermodynamic calculations for these temperatures.

The hardness of the alloys in the as-cast condition and in their three aged states was measured by Vickers indentations, and the results plotted together versus the carbon content in Figure 9. In the as-cast state the hardness increases with the carbon content from 2.5 (about 500Hv) to 3.5wt.% (about 650Hv), then stays almost constant between 3.5 and 5wt.%C. This evolution with carbon is seemingly the same after 50 hours of exposure at 1000 or 1100°C, but the hardness values after 50 hours at 1000°C are a little lower than for the as-cast states. In contrast the alloys have lost about 100 Hv after 50 hours at 1100°C. After exposure to 1200°C the measured hardness varies in the [400; 500Hv] range, without clear dependence on the carbon content.

General commentaries

In contrast with the nickel-based alloys earlier studied[8], which contain the same chromium and carbon contents, the cobalt alloys studied here are not all of a hyper-eutectic type. Both the matrix fractions and the chromium contents in matrix are lower than for the nickel alloys for the same carbon contents. This is a consequence of both the existence of the {high Cr/C atomic ratio}-Cr_7C_3 carbides in most of these cobalt alloys instead the {low Cr/C atomic ratio}-Cr3C2 carbides existing alone or with Cr_7C_3 in the nickel alloys. This is also due to the smaller presence of graphite in these cobalt alloys, by comparison with the nickel alloys, which promotes here the presence of more carbides and of more chromium involved in these carbides. As an example the lowest chromium content in matrix is here 4.4wt.%Cr in Co50 at 1000°C against 9.3wt.%Cr in the Ni-30Cr-5.0C alloy at the same temperature, according to Thermo-Calc. Thus, it appeared possible that the present cobalt alloys would be potentially more threatened by catastrophic oxidation than the corresponding nickel alloys, despite that the chromium contents in the whole alloys (30wt.%) meets the requirements for a chromia-forming behavior. Indeed it is not sure that the main part of these 30 weight percents of chromium, which was involved in the carbides during the microstructure formation - carbides which are rather coarse for some of them - may be released by the carbides' dissociation as quickly as required for combating oxidation. This limitation of chromium delivery, which threatened also the oxidation resistance of the nickel alloys, seems having had here more importance since many oxidized cobalt alloys are covered by spinel oxide, and even cobalt oxide in some cases, in addition to an inner chromia scale.

Nevertheless, if the coarsest carbides present in the hyper-eutectic cobalt alloys tended to do not dissolute and to be oxidized on site, the eutectic carbides disappeared from the external surface, leading to the development of a carbide-free zone, as for the nickel alloys. However, these two families of carbides-rich alloys did not behave similarly since the carbide-free depths after oxidation at 1000 or 1100°C are higher for these cobalt alloys than for the nickel alloys, especially for 1100°C, and for these ones especially for the alloys with the highest carbon contents: Co40, Co45 and

Full Paper

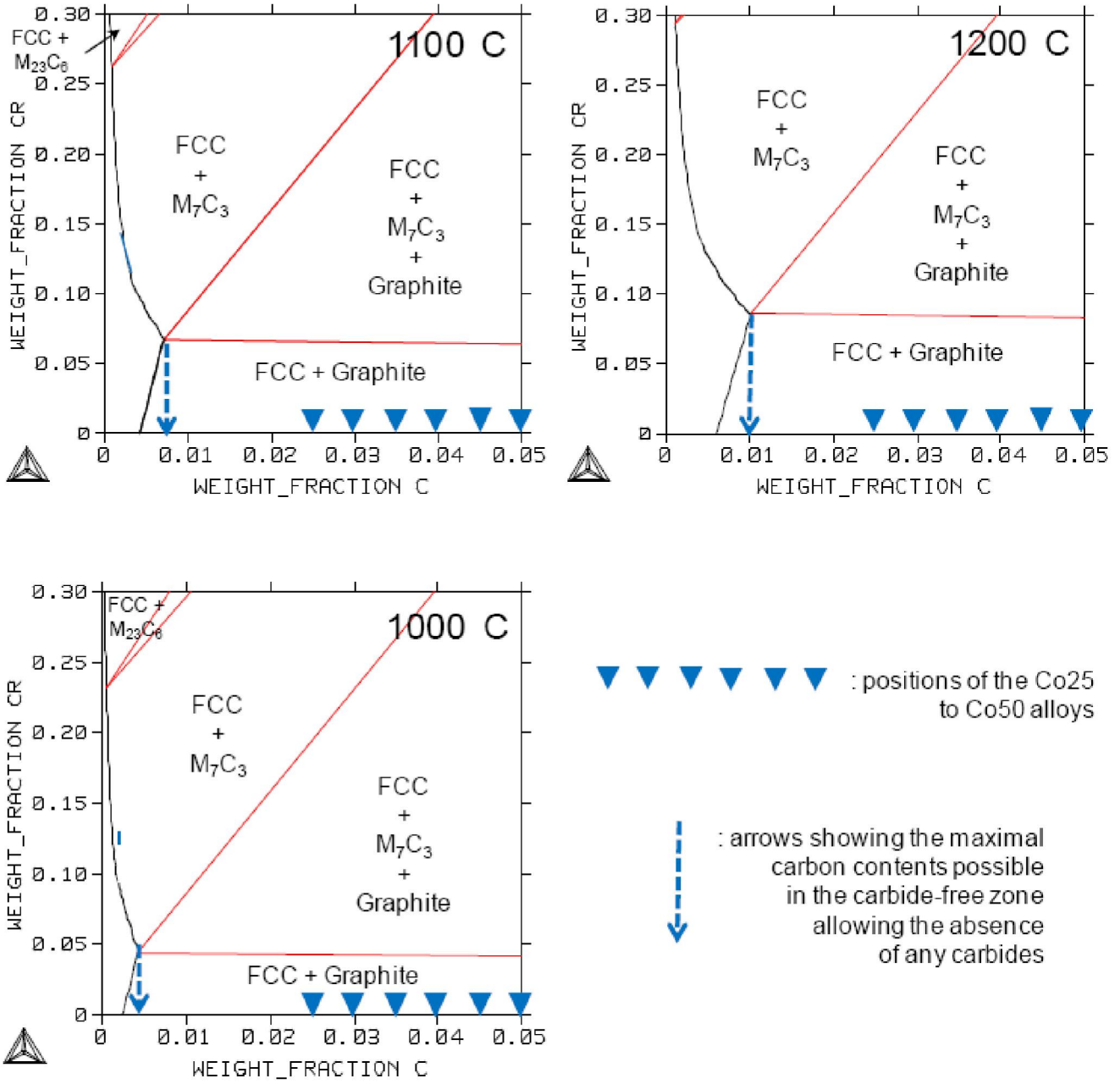

Figure 6 : Isothermal sections of the Co-Cr-C diagram computed with Thermo-Calc for determining the maximal local carbon contents compatible with the average chromium content and the absence of carbides in the carbide-free zones

Co50. The existence of other oxides than chromia as well as these deeper carbides-free zones demonstrated the worse chromia-forming behavior and the higher oxidation rate of these cobalt alloys by comparison with the nickel alloys with the same carbon contents. This is true again for oxidation at 1200°C since the carbide-free zones are also deeper for the Co25, Co30 and Co35 alloys than for the corresponding nickel alloys. The worse oxidation behavior of the cobalt alloys by comparison with the nickel alloys was also found in the case of the Co40, Co45 and Co50 alloys since their carbide-free depths after oxidation at 1200°C, which are much lower than for the nickel alloys but also significantly lower for the Co40, Co45 and Co50 alloys oxidized at 1100°C, clearly show that the oxide/alloy interface was moving inwards, and then that the whole alloys have started to be consumed by general oxidation. When the values of the carbide-free zones earlier obtained for cobalt-based 30wt.%Cr-containing ternary alloys with less carbon contents are added to the

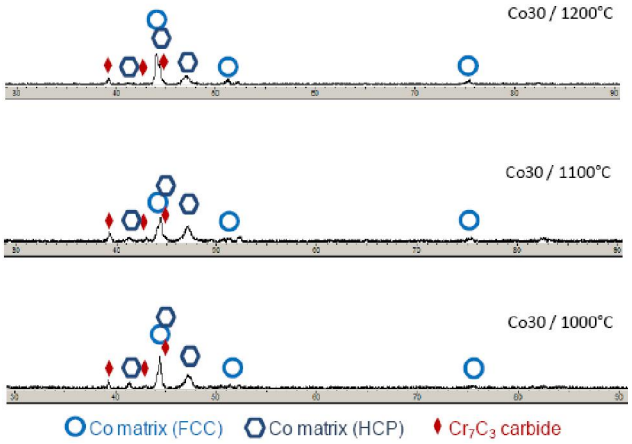

Figure 7 : X-ray diffraction spectra showing the natures of the carbides in the bulk of one of the C-lowest alloys of the study (Co30) after exposure to 1000°C, 1100°C and 1200°C

present values the graphs plotted in Figure 10(a) show a tendency of regular increase in depth of carbide-free zone for 1000°C, an increase too for 1100°C which is suddenly accentuated for the three highest carbon contents, and a very irregular dependence on the carbon content for 1200°C because of the very fast oxidation affecting some cobalt alloys among the richest in carbon. The nickel-based alloys[8] presented rather a slight decrease in carbide-free zone depth for an increasing carbon content, for all the three temperatures, and an abrupt increase with the carbon content only for the four carbon-richest alloys, revealing an acceleration of the oxidation rate but still without switching to catastrophic oxidation.

The chromium contents on the surfaces of the oxidized alloys are generally low, despite of the release of chromium by the carbides which have disappeared during oxidation, resulting in the development of the carbide-free zone. In most cases these contents are significantly lower than in the case of the nickel alloys with the same carbon contents and oxidized in the same conditions. In fact this is general between ternary cobalt alloys and the corresponding ternary nickel alloys since this order still remains when one adds previous results obtained for lower-carbon alloys in the same conditions of oxidation[20,21]. This can be seen by comparing the curves representing, for each of the three temperatures, the chromium contents on surface of the oxidized nickel alloys and the corresponding results obtained for the present cobalt alloys also plotted versus the carbon content in Figure 10(b). Indeed, if there is, for the two alloys' families, a more (nickel alloys) or less (cobalt alloys) regular decrease in surface chromium content over the [0; 5wt.%C] range for all temperatures, and also a more (nickel alloys) or less (cobalt alloys) systematic increase of this surface chromium content with temperature, the curves versus the carbon content for the nickel alloys tend to be above the ones corresponding to the cobalt alloys.

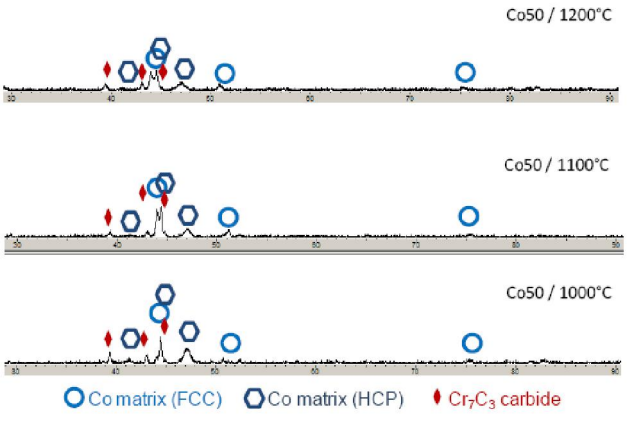

Figure 8 : X-ray diffraction spectra showing the natures of the carbides in the bulk of one of the C-richest alloys of the study (Co50) after exposure to 1000°C, 1100°C and 1200°C

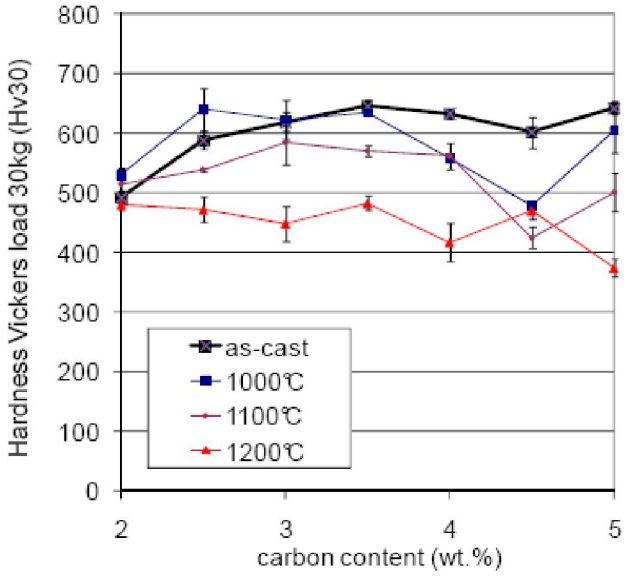

Figure 9 : Vickers hardness of the bulk of the as-cast alloys and of the oxidized samples

The deeper carbide-free zones and these lower chromium contents both show that oxidation was faster for the cobalt alloys than for the corresponding nickel alloys, and this can be confirmed by the quantities of chromium lost by the cobalt alloys which are higher than the chromium lost by the nickel alloys. There is how-

ever three exceptions: the chromium masses lost by cm^2 by the Co40, Co45 and Co50 alloys oxidized at 1200°C are, on the contrary, lower than for the nickel alloys with the same high carbon contents oxidized in the same conditions. This apparent inversion is only another consequence of the inward movement of the oxide/alloy interface induced by the general oxidation of these cobalt alloys. The same remarks and comparisons can be done concerning the carbon lost during oxidation, since this one is directly function of the carbide-free zone depth. The carbon quantities which were lost by the cobalt alloys obey also the same laws of increase with the bulk's carbon content in the alloy and with the temperature of oxidation, as the nickel alloys. The quantities assessed for the Co40, Co45 and Co50 alloys are here too seemingly lower than the real ones, consequence of the backward oxide/alloy interface. Due to the faster oxidation rates of these cobalt alloys by comparison to the nickel alloys, the lost carbon quantities are logically higher than the ones previously assessed for the nickel alloys for the same conditions.

In addition to surface deterioration the exposures to high temperature also induced changes in the bulk microstructures which were more significant for the highest temperature. As for the nickel alloys the morphologies of carbides evolved to minimize energy, with as consequence a slight softening of the alloys. For the present cobalt alloys the loss in hardness was a little higher than for the nickel alloys but all cobalt alloys remained harder than these ones whatever the temperature of exposure. This is due to the intrinsic higher hardness of the cobalt base and of the presence of more carbides and less graphite in the carbon-richest cobalt alloys.

CONCLUSIONS

By comparison with the high-carbon nickel-based alloys earlier studied, the present cast high-carbon cobalt-based alloys seem being better adapted to wear-resistant applications when only the mechanical properties are considered. The matrix of which is first intrinsically harder than the one of the nickel alloys, and second carbon is better used to enhance the hardness of such alloys. Indeed these cobalt alloys contain no or only low quantities of the carbon-consuming graphite and the carbides formed, lower in carbon, are present in higher quantities. These cobalt alloys are then harder than their corresponding nickel alloys, even after several hours spent at high temperature as it can be met in heat-producing friction uses. Unfortunately, such exposures to high temperature in oxidant atmospheres revealed that the oxidation behavior of the cobalt alloys is worse than the similar nickel alloys for such high carbon contents too. Oxidation induces also a surface deterioration which leads, at least to the development of a carbide-free zone, much softer than the initial alloy, which is therefore detrimental for the wear-resistance. Furthermore, in some cases, a catastrophic oxidation is possible. This threat is enhanced by the fact that the oxides scales may be logically periodically crushed and/or removed in service with as consequence an acceleration of the surface degradation. Thus, in the high temperature oxidation point of view, despite their mechanical superiority, these high carbon cobalt alloys must be considered to wear applications involving lower temperatures than for the corresponding nickel alloys.

ACKNOWLEDGEMENTS

The author wishes to thank E.Souaillat, O. Hestin, M. Ba and A. Dia for their contributions to this work, P. Villeger and Th. Schweitzer for their technical help, and also the Common Service of Microanalysis of the Faculty of Science and Technologies of Nancy.

REFERENCES

[1] D.A.Bridgeport, W.A.Brandtley, P.F.Herman; J.Prosthodontics, **2(3)**, 144 **(1993)**.
[2] C.T.Sims, W.C.Hagel; 'The superalloys', John Wiley & Sons, New York, **(1972)**.
[3] P.Berthod, J.L.Bernard, C.Liébaut, Patent WO99/16919.
[4] B.Roebuck, E.A.Almond; Int.Mat.Rev., **33(2)**, 90 **(1988)**.
[5] A.Klimpel, L.A.Dobrzanski, A.Lisiecki, D.Janicki; J.Mater.Proc.Technol., **1068**, 164-165 **(2005)**.
[6] G.V.Samsonov; 'Handbooks of high-temperature materials N°2. properties index', Plenum Press, New York, **(1964)**.
[7] D.Young; 'High temperature oxidation and corrosion of metals', Elsevier Corrosion Series, Amsterdam, **(2008)**.

[8] P.Berthod; Mater.Corros., In press.
[9] P.Kindermann, P.Schlund, H.G.Sockel, M.Herr, W.Heinrich, K.Görting, U.Schleinkofer: Int.J. Refract.Met.H., **17**, 55 **(1999)**.
[10] I.B.Panteleev, T.V.Lukashova, S.S.Ordan'yan; Powder Metall Met C+, **45(7-8)**, 342 **(2006)**.
[11] Thermo-calc version N: 'Foundation for computational thermodynamics' Stockholm, Sweden, www.thermocalc.com **(1993,2000)**.
[12] A.Fernandez Guillermet; Int.J.Thermophys., **8(4)**, 481 **(1987)**.
[13] J.O.Andersson; Int.J.Thermophys., **6(4)**, 411 **(1985)**.
[14] P.Gustafson; Carbon, **24(2)**, 169 **(1986)**.
[15] A.Fernandez Guillermet; Z.Metallkde, **78(10)**, 700 **(1987)**.
[16] J.O.Andersson; Calphad, **11(3)**, 271 **(1987)**.
[17] A.Fernandez Guillermet; Z.Metallkde, **79(5)**, 317 **(1988)**.
[18] P.Berthod, S.Michon, J.Di Martino, S.Mathieu, S.Noël, R.Podor, C.Rapin; Calphad, **27**, 279 **(2003)**.
[19] P.Berthod, C.Vébert, L.Aranda, R.Podor, C.Rapin; Oxidation of Metals, **63(1-2)**, 57 **(2005)**.
[20] P.Berthod; Annales de Chimie–Science des Matériaux, **33(3)**, 247 **(2008)**.
[21] P.Berthod, P.Lemoine, L.Aranda; Materials Science Forum, **595-598**, 871 **(2008)**.